In situ neutron diffraction studies of high density amorphous ice under pressure

2005 J. Phys.: Condens. Matter 17 S967

(http://iopscience.iop.org/0953-8984/17/11/029)

INSTITUTE OF PHYSICS PUBLISHING JOURNAL OF PHYSICS: CONDENSED MATTER

J. Phys.: Condens. Matter **17** (2005) S967–S974 doi:10.1088/0953-8984/17/11/029

In situ neutron diffraction studies of high density amorphous ice under pressure

Stefan Klotz[1,3], Th Strässle[1], A M Saitta[1], G Rousse[1], G Hamel[1], R J Nelmes[2], J S Loveday[2] and M Guthrie[2]

[1] Physique des Milieux Denses, IMPMC, CNRS UMR 7590, Université P M Curie, 4 Place Jussieu, 75252 Paris, France
[2] School of Physics and Centre for Science at Extreme Conditions, The University of Edinburgh, Edinburgh EH9 3JZ, UK

E-mail: stefan.klotz@pmc.jussieu.fr

Received 5 January 2005
Published 4 March 2005
Online at stacks.iop.org/JPhysCM/17/S967

Abstract

We review recent *in situ* neutron diffraction studies on the structural pressure dependence and the recrystallization of dense amorphous ices up to 2 GPa. Progress in high pressure techniques and data analysis methods allows the reliable determination of all three partial structure factors of amorphous ice under pressure. The strong pressure dependence of the $g_{OO}(r)$ correlation function shows that the isothermal compression of high density amorphous ice (HDA) at 100 K is achieved by a contraction (∼20%) of the second-neighbour coordination shell leading to a strong increase in coordination. The $g_{DD}(r)$ and $g_{OD}(r)$ structure factors are, in contrast, only weakly sensitive to pressure. These data allow a comparison with structural features of the recently reported 'very high density amorphous ice' (VHDA) which indicates that VHDA at ambient pressure is very similar to compressed HDA, at least up to the second-neighbour shell. The recrystallization of HDA has been investigated in the range 0.3–2 GPa. It is shown that hydrogen-disordered phases are produced which normally grow only from the liquid, such as ice XII, and in particular ice IV. These findings are in good agreement with results on quench-recovered samples.

(Some figures in this article are in colour only in the electronic version)

1. Introduction

When ordinary ice I_h is compressed at 77 K to 1.5 GPa it transforms to high density amorphous ice (HDA) [1]. This is the textbook example of a pressure-induced amorphization (PIA) of a crystalline solid and has been extensively studied in the past since it is believed to provide

[3] Author to whom any correspondence should be addressed.

key insights into the origin of PIA in general. PIA in ice is thought to be related to a lattice instability (phonon softening), as originally proposed by Tse *et al* [2] on the basis of molecular dynamics simulations. This suggestion is supported by our current experimental work on the phonon dispersion of ice I_h under pressure [3]. As for the nature of HDA, its low density counterpart LDA (low density amorphous ice) and the recently reported high density form VHDA (very high density amorphous ice), the situation is controversial. LDA is produced by heating HDA at ambient pressure to beyond ∼120 K, whereas VHDA is produced by heating HDA at 1–2 GPa to 160 K, i.e. close to the recrystallization temperature [4]. This phase is at ambient pressure ∼7% denser than HDA. The understanding of the relation among LDA, HDA and VHDA is a key issue in the current water debate. It was argued, for example, that HDA and LDA form the amorphous analogue of a two-phase liquid system below a liquid–liquid critical point at about 220 K [5]. This paper is devoted solely to structural studies on dense amorphous ice phases under pressure. We do not investigate relaxation phenomena occurring in HDA close to atmospheric pressure [6–8], indicating that a whole range of dense amorphous ice phases may occur in nature under these conditions. Although there is a substantial amount of literature on dense amorphous ices, all the structural work on HDA/VHDA to date is on the 'recovered' metastable forms, obtained after releasing the pressure back to ambient [6–8]. The present work arose out of an interest in the nature of HDA under pressure, and in particular the nature of the transformations of HDA to other crystalline ice forms [9]. This gave rise to the first *in situ* diffraction study of HDA, extending over the entire range of its existence, up to ∼2 GPa [10]. These studies were originally devoted to structural studies of HDA at ∼100 K under variable density, and then extended to VHDA after its discovery by Loerting *et al* [4]. The measurements became possible due to progress in high pressure methods using the Paris–Edinburgh cell [11], as well as data analysis techniques for disordered systems [12]. We show that it is indeed possible to obtain detailed and reliable structural data from a ∼80 mm^3 amorphous sample under pressure in the 0–2 GPa range.

The experiments reported here were performed on the PEARL station of the ISIS neutron facility at the Rutherford Appleton Laboratory (UK). HDA was produced by loading water (D_2O) into the Paris–Edinburgh high pressure cell equipped with sintered diamond (SD) anvils, cooling to 85 K to give ice I_h and then following with a slow compression at a rate of 1 GPa h^{-1}. The use of SD anvils is essential for this work because of its high transparency compared to conventional anvil material such as tungsten carbide. After data collection at 2, 0.7 and 0 GPa for typically 10 h each, the sample was carefully removed from the cell, and the gasket and anvils reassembled in exactly the same way to measure the background under strictly identical conditions, at the same temperature. The signal determined in this way was subtracted from the overall signal (b/s ratio typically 10%). The diffraction patterns were then corrected for the wavelength-dependent attenuation due to the anvil material (sintered diamond), as is done in standard measurements using this high pressure cell [13]. The patterns obtained in this way at 0 GPa are in excellent agreement with the best available atmospheric pressure $S(Q)$ data published by Bellissent-Funel (inset figure 1) [14]. The data are free from any contaminant scattering from the pressure cell materials and, although the small sample volume limits the statistical precision, it can be seen that there is excellent agreement with [14]. These patterns indicate significant structural modifications: at 2 GPa, the main peak has shifted to lower d-spacings by ∼0.3 Å and reduced by ∼30% in width.

It is not possible to determine the pressure directly in our measurements. The pressure values quoted here (0.7 and 2 GPa) were determined in separate runs using HDA samples mixed with non-transformed ice I_h or ice VII (to which HDA transforms beyond ∼2.5 GPa), by calibrating the position of the strongest diffraction feature of HDA at ∼2.6–3.0 Å using the known equations of state of these crystalline ice phases. The density of HDA, the relevant

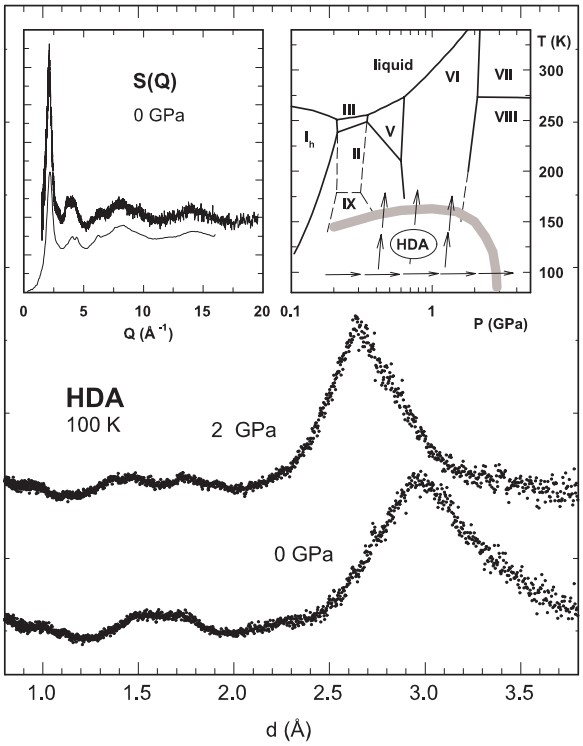

Figure 1. The principal peak in neutron diffraction patterns from HDA at 0 and 2 GPa (main figure, dots). The inset on the left compares the complete 0 GPa data (upper plot) with published ambient pressure $S(Q)$ data [14] plotted as a function of $Q = 2\pi/d$. The inset on the right shows the phase diagram of water, including the domain of existence of HDA. The broad line shows schematically the recrystallization temperature and dashed lines are extrapolated phase boundaries. The arrows show the P–T paths followed in the recrystallization experiments described in the text.

parameter for the data analysis, was then determined from published p–V measurements to 1 GPa [1, 15], extrapolated to 2 GPa. The estimated errors in pressure are ± 0.1 GPa at 0.7 GPa and ± 0.2 GPa at 2 GPa, a precision which is sufficiently good for the interpretations of the results reported here.

The data were then analysed by a Monte Carlo refinement technique (empirical potential structure refinement [16, 12], EPSR), a method which was successfully applied previously for the analysis of low and high density water [16, 12] as well as LDA and HDA [17]. EPSR makes use of realistic intramolecular and intermolecular potentials (in this case SPC/E) to constrain the configurations in a simulation box containing typically 1000 molecules. An empirical potential is generated from the difference between measured and calculated structure factors and successively refined as the molecules are moved to give the best possible fit with the diffraction data. For water, the choice of a specific potential (SPC/E, SP10) was shown to have only a minor influence on the results [12] indicating that the conclusions reported here are independent of simulation details. Compared to simple Fourier transform methods, EPSR has the advantage of providing all three partial correlation functions $g_{\alpha\beta}(r)$ and the three-dimensional distribution around a given D_2O molecule. EPSR is also free from truncation artefacts that are inherent to Fourier transformation methods. A detailed description of this method can be found elsewhere [16, 12].

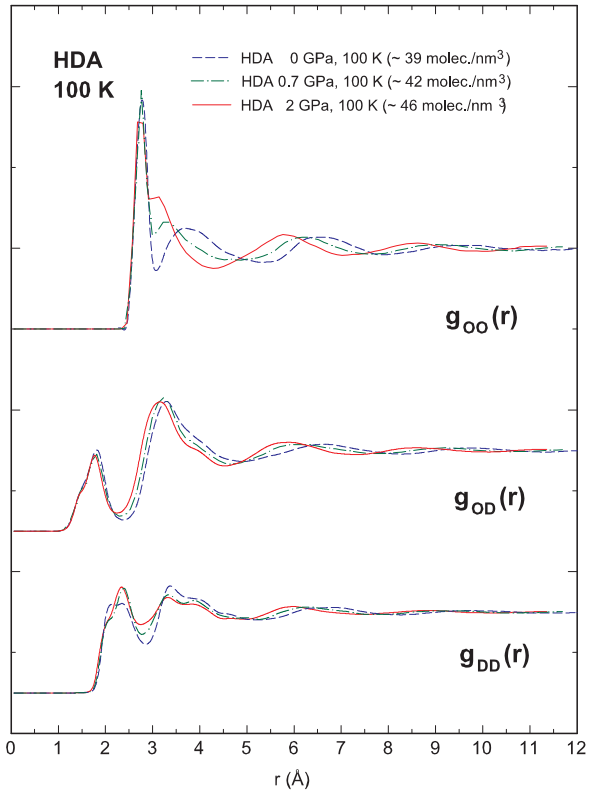

Figure 2. Site–site radial distribution functions $g_{\alpha\beta}(r)$ of HDA at 0, 0.7 and 2 GPa. The first peaks in $g_{\mathrm{OD}}(r)$ (at ∼1.8 Å) and $g_{\mathrm{DD}}(r)$ (at ∼2 Å) are, respectively, the D···O hydrogen bond length and the intermolecular D–D distance. The strong intramolecular contributions to $g_{\mathrm{OD}}(r)$ and $g_{\mathrm{DD}}(r)$ at 1.0 and 1.5 Å have been subtracted for clarity.

Figure 2 shows the results for the refined $g_{\alpha\beta}(r)$. Out to the first peak in $g_{\mathrm{OO}}(r)$, the features are all those expected for tetrahedral H bonding, with an O···O distance of ∼2.8 Å, and these features show no significant change with pressure. However, the second peak in $g_{\mathrm{OO}}(r)$ at ambient pressure is centred at 3.7 Å rather than at 4.5 Å expected for second-neighbour tetrahedral bonding, as seen in LDA, ice $\mathrm{I_h}$ and low density water [17]. This peak moves rapidly to even lower r with pressure so that by 2 GPa it becomes a shoulder on the first peak at 2.8 Å. The third and fourth peaks also move strongly to lower r with pressure. Integrations of $g_{\mathrm{OO}}(r)$ reveal that there are about 12 molecules over the range 3.1–4.6 Å at ambient pressure, as expected for the second coordination shell. As this second peak moves to shorter r with increasing pressure, fewer molecules are associated with it. At 2 GPa integration of $g_{\mathrm{OO}}(r)$ to 3.5 Å gives a coordination number of 9.0(2) suggesting that, in addition to the four molecules of the unchanged first shell at 2.8 Å, a further about five molecules are associated with the main part of the shoulder that remains from the initial second peak. Integration of $g_{\mathrm{OO}}(r)$ from 3.5 to 4.6 Å reveals that there are another about eight molecules in this region. Compared to these significant changes seen in $g_{\mathrm{OO}}(r)$, the two other correlation functions, $g_{\mathrm{OD}}(r)$ and $g_{\mathrm{DD}}(r)$, exhibit only a weak pressure dependence.

Figure 3 gives an idea of the three-dimensional arrangement of molecules (oxygen atoms) around a molecule with given orientation ('spatial distribution function', SDF). These

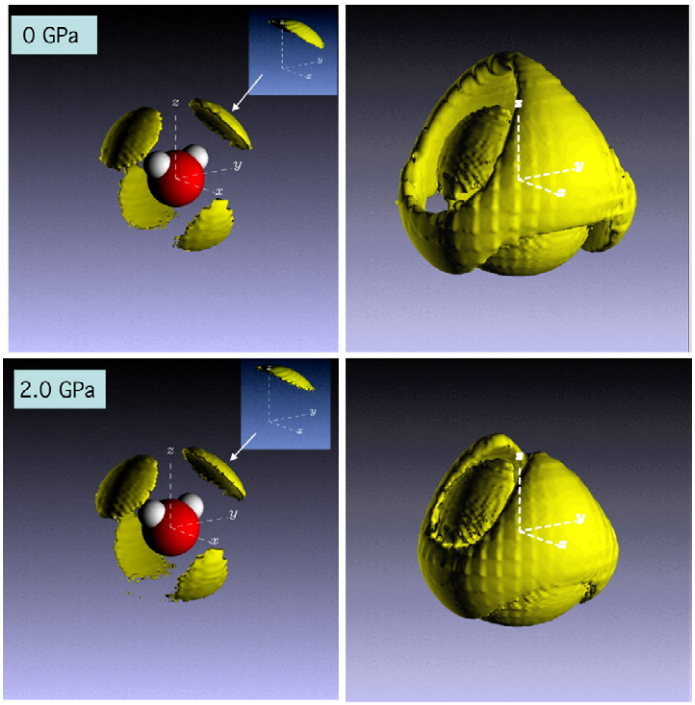

Figure 3. Spatial distribution functions (SDFs) of the oxygen atoms of HDA. The upper plots were obtained from data collected at 0 GPa and show (left) the density in the range 2.0–3.1 Å (the first coordination shell) and (right) that for the range 2.0–4.8 Å (the first and second coordination shells). The lower plots, from data collected at 2 GPa, show (left) the density in the range 2–3.0 Å and (right) that for the range 2.0–4.3 Å. The levels of all isosurfaces have been set to enclose 40% of the molecules within the specified ranges.

are isosurfaces of the oxygen probability distribution. The figure indicates that the first coordination shell (left panels) is essentially tetrahedral, as expected, and that the form and radius of this shell are pressure independent. The second-shell SDF (right panels) forms another approximately tetrahedral arrangement, inverted with respect to that of the first shell. Though the spatial arrangement of this tetrahedron is unaffected by pressure, its radius shrinks rapidly, as $g_{OO}(r)$ shows, and approaches the radius of the first shell at 2 GPa.

The question arises as to how the first and second shells are connected given the short and very pressure-dependent second-shell distance. The distance from second-neighbour to first-neighbour molecules at more than 3.5 Å is too long to be an H bond. Thus, the majority of the second-shell molecules cannot donate H bonds either towards the original molecule or towards the first-shell molecules. This is also the conclusion derived from previous ambient pressure data [17], which show that the fifth interstitial molecule was not bonded to the central molecule.

HDA is essentially fourfold coordinated at ambient pressure when molecules up to the first minimum ($r = 3.05$ Å) in $g_{OO}(r)$ are considered, with a broad shell of some 12 molecules beyond. Under pressure, the coordination increases drastically with four H bonded neighbours and 4–5 non-bonded neighbours at 2 GPa (r up to 3.5 Å). This interpretation is consistent with the Finney *et al* observation of a fifth, interstitial, molecule at ambient pressure [17], since their conclusion is based on integration out to 3.3 Å. Our results reveal that this fifth

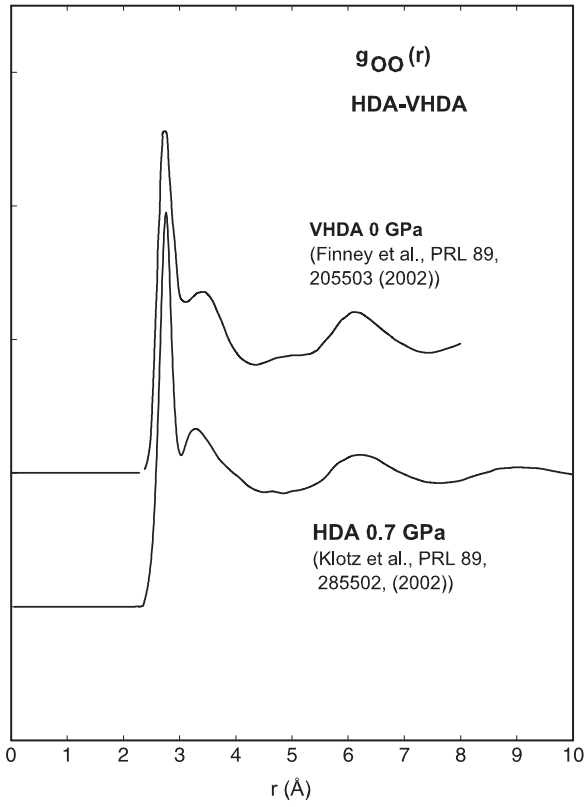

Figure 4. Comparison of $g_{OO}(r)$ radial distribution functions of VHDA at ambient pressure [18] with those obtained in this work on HDA at 0.7 GPa [10].

molecule and the associated patches in the SDFs in [17] are in fact the short r part of the broad second shell.

These pressure data allow an interesting comparison of the correlation functions of HDA and VHDA at approximately the same density. For this purpose we take the published ambient pressure data for VHDA obtained at 0 GPa [18] and compare them to our data for D_2O HDA collected at 0.7 GPa (as already shown in figure 2). Under these conditions, the two systems have approximately the same molecular density, i.e. 0.07 mol cm^{-3}. Figure 4 shows the remarkable similarity of the O–O correlation functions, indicating that the basic mechanism of densification in VHDA (occurring between 100 and 160 K) is the same as the pressure-induced densification at 100 K, and that the structures up to second-neighbour distances are essentially identical. Nevertheless, HDA returns to its original density when decompressed at 80 K, whereas VHDA remains permanently densified. The microscopic origin for this difference is without doubt subtle and difficult to detect in diffraction experiments. This issue is still under debate [19, 20].

In order to gain a deeper insight into the mechanism of densification when going from HDA to VHDA we have carried out classical molecular dynamics simulation based on the TIP4P potential [20]. These calculations where run for a temperature of 160 K and benchmarked to *in situ* neutron diffraction data obtained at 1.8 GPa at approximately the same temperature, giving excellent agreement in the O–O partial correlation function. The advantage of these simulations is that VHDA can be 'supercompressed' to beyond its experimentally known

stability domain (i.e. 2.5 GPa), thereby revealing more clearly the subtle structural trends occurring under pressure. It turns out that an interesting structural detail to consider is the distribution of the six O–O–O angles in the first-neighbour cage. For LDA this distribution is centred at the tetrahedral angle of 109.5°, as expected. For HDA, this distribution becomes broader due to the increasing angular distortions, but remains otherwise featureless. In VHDA, in contrast, the distribution shows shoulders which develop into distinct peaks at 60°, 120° and 180° when VHDA is supercompressed to 1.9 g cm^{-3}. The occurrence of these features can be interpreted as a trend towards a random close packed structure. It was pointed out that the topology of HDA under pressure, which contains ∼9 molecules up to ∼3.5 Å, resembles locally the eightfold-coordinated ice VII/VIII structure [10]. However, the above simulations indicate that if structural trends upon compression at higher temperatures (160 K) are considered, amorphous ice develops more towards a random close packed arrangement, a configuration which is nevertheless compatible with the hydrogen bonding in water [20].

A further interesting observation arising from our *in situ* diffraction measurements concerns the unexpected recrystallization behaviour of dense amorphous ice under pressure, i.e. VHDA according to the current terminology [9]. When warmed at different pressures between 0.3 and 2 GPa, HDA crystallizes, in order of pressure, into ices III, IV, V, XII, VI and VII [21, 9], and not into the equilibrium forms found under these conditions. This behaviour was also reported on quench-recovered samples [4, 22]. A particularly intriguing observation is the clear absence of ice II in all the recrystallization experiments reported so far, our own ones and those of the Innsbruck group [23]. It thus appears that HDA/VHDA crystallizes into the same phases as would be formed on cooling liquid water at a similar density. It is difficult to derive any further structural conclusions on the basis of such recrystallization data. But it appears that if HDA/VHDA were composed of nanocrystalline ice phases as has been proposed [24], there should be a sizable fraction of ice II given the large stability field of this phase at low temperatures. This phase should then be found in the recrystallized samples, which is however not the case. A Rietveld analysis of HDA/VHDA spectra shows that if any crystalline phase is present in such samples, the only realistic candidates would be ice III/IX and ice XII, but with grain sizes below ∼2 nm. Obviously it makes little sense to define a unit cell over a such a length scale, and we conclude that there is no evidence that HDA/VHDA is other than amorphous on the basis of our diffraction data.

Some of the features observed in amorphous ices, such as the phenomena of permanent densification and the structural relaxation at high and low pressures, are common to related amorphous forms, such as amorphous SiO_2 and GeO_2. It would be interesting to investigate the structural pressure dependence and the recrystallization behaviour of these systems at a similar level of detail to that in these studies of ice. This would yield important insight into the physics of random network amorphous solids in general.

Acknowledgments

We acknowledge a close and fruitful collaboration with A Soper on the data analysis using the EPSR algorithm, as well as thanking D J Francis for assisting in the experiments. Our work (JSL, MG, RJN) was funded by a research grant from EPSRC, and supported by CCLRC through access to beamtime and other resources. One of us (TS) would like to acknowledge a grant (81EZ-68588) from the Swiss National Science Foundation.

References

[1] Mishima O, Calvert L D and Whalley E 1984 *Nature* **310** 393
[2] Tse J S *et al* 1992 *J. Chem. Phys.* **96** 5482

[3] Strässle Th, Klotz S, Saitta A M and Braden M 2004 *Phys. Rev. Lett.* **93** 225901
[4] Loerting T, Kohl I, Salzmann C G, Mayer E and Hallbrucker A 2002 *J. Chem. Phys.* **116** 3171
[5] Mishima O and Stanley H E 1998 *Nature* **396** 329
[6] Koza M M, Schober H, Fischer H E, Hansen T and Fujara F 2003 *J. Phys.: Condens. Matter* **15** 321
[7] Tulk C *et al* 2003 *Science* **297** 1320
[8] Guthrie M *et al* 2003 *Phys. Rev.* B **68** 184110
[9] Klotz S, Hamel G, Loveday J S, Guthrie M and Nelmes R J 2003 *Z. Kristallogr.* **218** 117
[10] Klotz S, Hamel G, Loveday J S, Guthrie M and Nelmes R J 2002 *Phys. Rev. Lett.* **89** 285502
[11] Besson J M, Hamel G, Weill G, Nelmes R J, Loveday J S and Hull S 1992 *Physica* B **180/181** 907
[12] Soper A K 2000 *Chem. Phys.* **258** 121
[13] Wilson R M, Nelmes R J, Loveday J S, Klotz S and Marshall W G 1995 *Nucl. Instrum. Methods* A **354** 145
[14] Bellssent-Funel M-C, Teixeira J and Bosio L 1987 *J. Chem. Phys.* **87** 2231
[15] Mishima O, Calvert L D and Whalley E 1985 *Nature* **314** 76
[16] Soper A K and Ricci M A 2000 *Phys. Rev. Lett.* **84** 2881
[17] Finney J L, Hallbrucker A, Kohl I, Soper A K and Bowron D T 2002 *Phys. Rev. Lett.* **88** 225503
[18] Finney J L, Bowron D T, Soper A K, Loerting T, Mayer E and Hallbrucker A 2002 *Phys. Rev. Lett.* **89** 205503
[19] Martnak R, Donadio D D and Parrinello M 2004 *Phys. Rev. Lett.* **92** 225702
[20] Saitta A M, Strässle Th, Rousse G, Hamel G, Klotz S, Nelmes R J and Loveday J S 2004 *J. Chem. Phys.* **121** 8430
[21] Klotz S, Hamel G, Loveday J S, Guthrie M and Nelmes R J 2001 *ISIS2000—Rutherford Appleton Report* 2000-2001, ER 12206
[22] Salzmann C G, Loerting T, Kohl I, Mayer E and Hallbrucker A 2002 *J. Phys. Chem.* B **106** 5587
[23] Salzmann C G, Mayer E and Hallbrucker A 2004 *Phys. Chem. Chem. Phys.* **6** 5156
[24] Johari G P 2000 *Phys. Chem. Chem. Phys.* **2** 1567